

C. Polacsek, R. Barrier

(Onera)

M. Kohlhaas, T. Carolus

(Institute for Fluid and Thermodynamic)

P. Kausche, A. Moreau

(DLR)

F. Kennepohl

(MTU Aero Engines)

E-mail: cyril.polacsek@onera.fr

DOI : 10.12762/2014.AL07-03

Turbofan Interaction Noise Reduction Using Trailing Edge Blowing: Numerical Design and Assessment and Comparison with Experiments

This paper investigates the effect of a flow control device on turbofan sound generation, applied to a low-speed axial compressor model in a laboratory test rig. This treatment consists in a secondary mass flow ejected through the trailing edge of the rotor blades, designed to fill the velocity defect behind the rotor and to decrease the turbulent kinetic energy related to the wakes, so that broadband interaction noise should be reduced. The design and implementation of the blowing device is first briefly described, as well as the fan stage experiment. Then, the paper focuses on computation methods devoted to the capture of turbulent wakes and to the acoustic response of the stator (with and without blowing). 3D steady RANS and quasi-2D LES approaches are considered for the CFD, both coupled to an integral formulation based on the theory proposed by Amiet, aiming at calculating the in-duct sound power and estimating the acoustic performance of the treatment. Under optimal blowing conditions, significant sound power reductions are predicted by the simulations. First attempts to relate numerical predictions to available measurements, *i.e.*, hot-wire data and in-duct sound power spectra, are proposed and discussed.

Introduction

A major source of broadband turbofan noise results from the interaction of turbulent rotor blade wakes with the outlet guide vanes (OGV). The objective of this study is to assess the effect of a flow control device on sound generation, applied to a low-speed axial compressor model in a laboratory test rig and studied within the framework of the European project FLOCON. This treatment consists in a secondary mass flow ejected through the trailing edge of the rotor blades (Trailing Edge Blowing, TEB). It is designed to fill the velocity defect behind the rotor and to decrease the turbulent kinetic energy related to the wakes, so that interaction noise should be reduced. Tone noise reduction has been successfully investigated by Brookfield and Waitz [1] and by Sutliff et al. [2], with optimal PWL tone reduction measured in the NASA Glenn Aero-Acoustic Propulsion Laboratory (AAPL) of 5.4, 10.6, and 12.4 dB for the first three tones, respectively. Further investigations by Sutliff [3] focused on broadband noise, showing a 2-3 dB average reduction on the turbulent pressure spectrum measured over the stator vane surface. However, only 1 dB attenuation of broadband PWL in the aft arc was assessed by far-field measurements for optimal blowing rate, probably due to the rotor noise dominating the contribution in the Advanced

Noise Control Fan (ANCF) test bed. Noise benefits of rotor TE blowing have been also investigated on an advanced model turbofan tested in the NASA Glenn 9- by 15-Foot Low Speed Wind Tunnel (9x15 LSWT) [4], confirming the acoustic performance of the TEB for the tones and indicating some broadband noise reductions, possibly attributed to a reduction of blade wake turbulence.

Another attempt is investigated here on a laboratory test rig with similar TEB technology and using extensive numerical simulations, focusing on the broadband noise component and only considering outlet duct acoustic measurements. Previous studies [5] showed that, for most loaded OGV conditions, the broadband sound power measured in the outlet duct was mainly attributed to the rotor-stator interaction mechanism. Compared to the 1.2 m diameter turbofan simulator used in [3], this laboratory experiment is quite limited by the size of the rig (0.45 m rotor diameter) and then by the thickness of the vanes (very thin) at the trailing edge. Thus, practical blowing mass flow rates can only be reached by increasing the jet velocity. As pointed out in [6], the turbulent mixing of high-speed blowing jets can cause additional broadband noise sources that might increase the PWL spectrum (particularly the high-frequency part), as is also discussed in this paper.

The design and implementation of the blowing device performed by the USI (University of Siegen), already detailed in a more dedicated communication [7], is first briefly described here, as well as the fan stage experiment. Then, the paper focuses on computation methods devoted to the capture of turbulent wakes and to the acoustic broadband response of the stator (with and without blowing). 3D steady RANS and quasi-2D LES approaches are considered for the CFD, both coupled to an integral formulation based on the theory proposed by Amiet, aiming at calculating the in-duct sound power and estimating the acoustic performance of the treatment. Although restricted to a thin radial extent, LES permits the turbulence spectrum content and the integral length scale to be locally assessed. These methodologies and the resulting blowing effect on turbulence characteristics and acoustic behavior are addressed. First attempts to relate numerical predictions to available measurements, *i.e.*, hot-wire data and in-duct sound power level (SPL) spectra are discussed.

Fan stage model and trailing edge blowing implementation

The measurements were performed in a laboratory scale fan rig located at DLR Berlin. For the design and the implementation of the blowing devices, a new fan with 18 blades containing internal passages for TEB was designed. Important design parameters are given in table 1 and figure 1. Two x-hot-wire probes located downstream of the rotor trailing edge plane are used to measure the wake characteristics and a microphone rake provides the acoustic spectra in the outlet duct.

Volume flow rate at the inlet \dot{V}_{in}	2.52	[m ³ /s]	Rotor speed, N	3159	[rpm]
Rotor diameter D_A	0.4524	[m]	No. of rotor blades, B	18	
Hub diameter D_I	0.286	[m]	No. of stator vanes, V	32	

Table 1 – Design parameters of the fan stage

For the rotor blade design, a NACA 6515-63 airfoil with span length $L_{span} = 83.2$ mm is used. The fan operates at its design flow rate coefficient:

$$\phi_{in} \equiv \frac{\dot{V}_{in}}{\pi^2 D_A^3 N} = 0.21 \quad (1)$$

The position of the reference plane corresponds to the stator leading edge. The wake velocity profiles and the turbulent quantities are evaluated at a relative blade height of:

$$h^* = \frac{h}{(D_A - D_I) / 2} \quad (2)$$

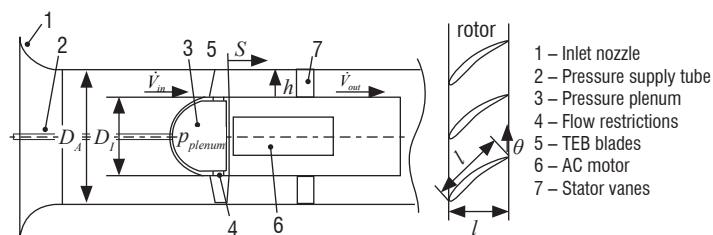


Figure 1 – Schematic drawing of the TEB fan stage: meridional section (left) and coaxial section of the cascade (right)

Figure 2 shows the internal passages with guide vanes, shaped carefully to avoid excessive pressure losses. The internal passages responsible for a specific blade height are connected to the pressure plenum in the hub via flow restrictions, which control the individual blowing mass flow rates. The inlet cross sections of the restrictions, as well as the plenum pressure, were optimized claiming a flat wake velocity profile. A pressure supply tube from the inlet nozzle to the plenum delivers the needed pressure, as well as the overall TEB mass flow.

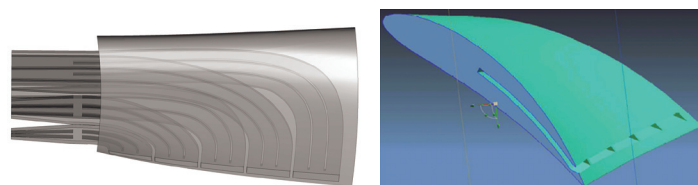


Figure 2 – Rotor blade with internal passages, guide vanes and flow restrictors at the passage entrances (left), and CAD geometry (right) provided by the USI

RANS-based and LES-based methodologies

3D RANS computations (USI)

RANS computations are mainly performed by the USI. The computational domain consists of 1/18th of the bladed annulus, from 1.0 D_A upstream to 1.0 D_A downstream of the rotor. It also covers the five internal blade passages including the guide vanes, from their inlet in the hub to their orifices, where the jet flow mixes with the main flow. General grid interface (GGI) boundary conditions were imposed in the circumferential direction. The inlet mass flow rate of the fan system was imposed on the upstream boundary according to the operation point of $\phi_{in} = 0.21$, while an opening pressure boundary condition was set at the downstream boundary. At the entrance of each of the five internal blade passages, the flow restrictions and the pressure plenum inside the hub were modeled. Of course, no boundary conditions have to be specified at the exit of the channels (*i.e.*, the orifices), since the flow mixes with the main flow. To solve the RANS equations, ANSYS CFX with the standard SST-turbulence model and a 2nd order approximation (blend factor of 1) was employed [8]. The block structured numerical grid consists of 7.1 million nodes. Special attention was paid to the wake region, by using a very fine grid resolution of about 3 million nodes. Common grid quality criteria were considered in most of the fluid flow regions (grid angles > 20°). Due to geometrical restrictions, some grid angles in the TEB injection orifices were as small as 13°. In these regions, a finer grid was employed to ensure sufficient accuracy. For the simulation, the maximum value of y^+_{max} for the first node adjacent to the blade surface was < 6, whereas the area averaged y^+_{ave} at the blade was < 1. The convergence criteria were set to 1.10⁻⁶ MAX residuals.

3D RANS and quasi-2D LES computations (Onera)

3D RANS computations have been also performed on a baseline case, using the CFD Onera code elsA that solves the compressible equations in the relative frame with a cell-centered finite volume formulation. Space discretization is ensured using the Jameson second-order-centered scheme with the addition of an artificial viscosity. Turbulence closure is achieved using the $k-l$ turbulence model proposed by Smith [9]. In this model, l (characteristic length scale of turbulence) is a transported quantity. The computation is performed on a single rotor passage using a multi-block grid of about 1 million nodes. Particular attention has been paid to the mesh downstream of the blade, to keep

a good description along the wake development zone. The mesh has 17 cells in the rotor tip gap. The exit plane is located approximately at 3 chord lengths from the rotor trailing edge.

Due to CPU and memory limitations, the LES approach is practically restricted to a quasi-2D computation [10,11] so that the simulation is only focused here on a thin strip (L_{strip}) of the full spanwise response. As in reference 10, the sub-grid scale viscosity is given by the WALE model (Wall Adapting Local Eddy-viscosity) [12]. The quasi-2D computation domain is a section in a circumferential plane at mid-span (corresponding precisely to a half height of the central injection slit for the blowing case) and extruded in the spanwise direction over 20% of the chord (figure 3, left). The full 3D test-case is thus converted to a cascade-like test-case for the LES simulation, assuming that flow physics of the fan rig remains well captured by this conversion. In the LES simulation, the incoming flow is perfectly laminar. Any "background" turbulence thus comes only from the unsteadiness created in the simulation (that is, from shear, even small, outside the boundary layer and the wake zone). The mesh size (Δx , Δy , Δz) near the airfoil must verify some criteria for the validity of the LES computation. The non-dimensional criteria used for this study are: $\Delta x^+ \leq 40$, $\Delta y^+ \leq 2$, $\Delta z^+ \leq 20$.

The blowing mass-flow in the central injection slit obtained from a 3D computation (USI) is translated in the quasi-2D LES as an equivalent mass-flow, by using uniform blowing along the entire extrusion of the blowing slit (figure 3, right). Optimal blowing conditions issued from USI computations were obtained with $\dot{m}_{blowing} = 142$ g/s.

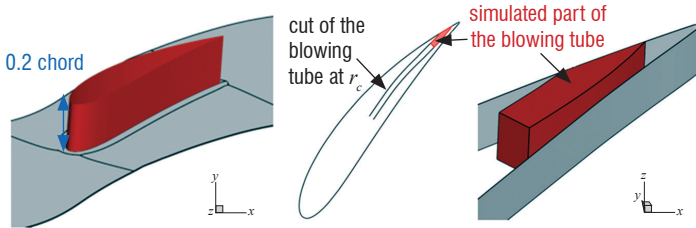


Figure 3 – LES spanwise extrusion (left) and simulated part of the blowing tube (right)

Acoustic post-processing based on the Amiet broadband noise theory

This section presents the Amiet-based theory [13] adopted here to predict broadband interaction noise, using either 3D RANS or 2D LES output data. A concise form of Onera formulation [14] providing the power density spectrum (PSD) of the acoustic power, S_{ww} , in the outlet duct can be written as:

$$S_{ww}(f) = V \sum_{m=-m_{max}}^{+m_{max}} \sum_{n=1}^{n_{max}} \varphi_{mn}(r_s, f) |\mathcal{L}(r_s, K_c, 0)|^2 U_c \phi_{u_n u_n}(K_c, 0) \quad (3)$$

φ_{mn} is a kernel function related to the Green function (valid for an annular duct and a uniform mean flow), \mathcal{L} is the aeroacoustic transfer function obtained from the aerodynamic response of an isolated (zero-thickness) stator vane. K_c and U_c are respectively the convection wave-number and the convection speed, taken equal to the streamwise velocity (U_s). $\phi_{u_n u_n}$ is the 2-wavenumber turbulence

spectrum related to the upwash velocity component, u_n , and adjusted using standard Von-Karman model. $\phi_{u_n u_n}$ can be expressed versus the turbulent velocity spectrum, $S_{u_n u_n}$ and the spanwise correlation length scale, ℓ_y :

$$\phi_{u_n u_n}(K_c, 0) = \frac{U_c}{\pi} S_{u_n u_n}(\omega) \ell_y(\omega) \quad (4)$$

$\phi_{u_n u_n}$ requires the knowledge of the mean-square turbulent velocity, u_{turb} (also related to the kinetic energy, k) and the integral length scale, Λ . This information is usually obtained from a RANS calculation. In (4), the upwash turbulent velocity spectrum and spanwise correlation length scale may be directly post-processed from LES output data, as done here for $S_{u_n u_n}$. However, assessment of ℓ_y is practically not feasible, because the radial extent is too thin. An alternative approach is to use an analytical expression for ℓ_y , deduced from the Von-Karman spectrum and directly related to Λ , as discussed by Lynch [15]. CFD data extraction for RANS and LES output post-processing is sketched in figure 4. The inter-stage red plane in figure 4 (left) corresponds to the hot-wire position in the DLR rig. Inputs to (4) are taken at the stator leading edge (LE) position. In figure 4 (right), LES data is interpolated from the rotating frame to the fixed frame and uniformly distributed along a mean streamline assumed to represent the path of convected turbulent structures impacting the stator vane (chord aligned to this path). This allows us to calculate the turbulent velocity spectra and the integral length scale at mid span.

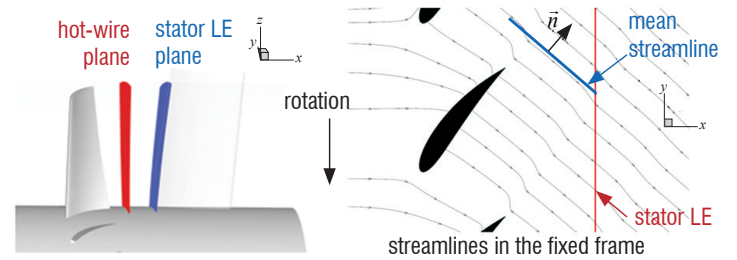


Figure 4 – CFD data extraction for aeroacoustic analyses: 3D RANS (left) and quasi-2D LES (right)

Aerodynamic and noise predictions, and comparison with experiment

Rotor wake characteristics

Firstly, wake characteristics in terms of velocity defect and turbulence intensity have been analyzed, in order to check the reliability of the CFD computations (by comparison to the experiment in a baseline case) and to estimate the effect of the blowing. Axial velocity profiles computed by USI RANS are compared to the measurements for two spanwise stations in figure 5. Predicted and measured blowing effects are similar, showing a significant reduction at 74% span but an overshoot at 44% span, revealing quite important radial effects. Although optimal blowing conditions assessed by RANS were estimated using a minimization process at several radial stations, wake filling performances achieved by a blowing distribution through the five slits and measured by the hot-wire probes reveal significant differences (compared to the simulations), particularly when moving towards the casing.

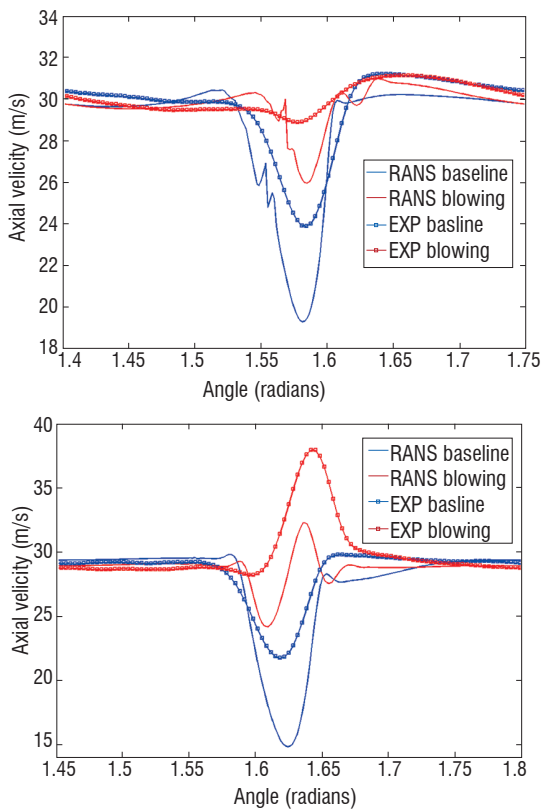


Figure 5 – Axial velocity profiles issued from USI RANS and experiment at 74% (top) and 44% (bottom) span

Turbulence intensity, T_u , scaled by axial, radial and tangential velocity components is defined as:

$$T_u = \frac{u_{turb}^{1/2}}{U_s} = \frac{u_{turb}^{1/2}}{\sqrt{U_x^2 + U_r^2 + U_t^2}} \quad (5)$$

$$u_{turb} = \frac{1}{3} (\langle u_x^2 \rangle + \langle u_r^2 \rangle + \langle u_t^2 \rangle) = \frac{2}{3} k$$

T_u 360°-plots issued from USI RANS baseline computation (1 rotor blade channel) and from baseline and blowing experimental cases (18 blade passages) are compared in figure 6. The agreement between prediction and measurements is rather good, although the turbulent wake level is over estimated by RANS. Intense turbulence spots near the hub and casing can be also observed in the experiments. Measured T_u wakes are clearly attenuated when the blowing is active (figure 6, right), despite slight blade-to-blade irregularities. This effect is highlighted in figure 7, comparing the T_u plots over 1 blade channel (time-averaging using blade passing trigger in the experiment). The reduction of turbulence intensity due to the blowing is fairly well assessed by the CFD, but the levels are overpredicted, except near the blade foot region, where the measurements are higher.

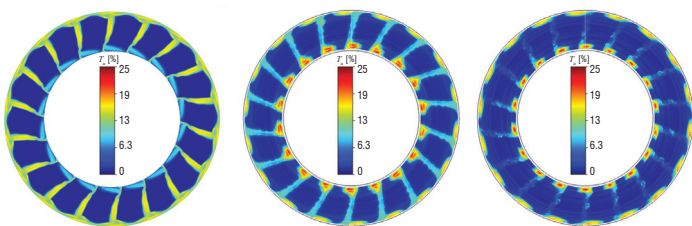


Figure 6 – Turbulent intensity plots: RANS-SST (baseline, left) and exp. (baseline, mid. and blowing, right)

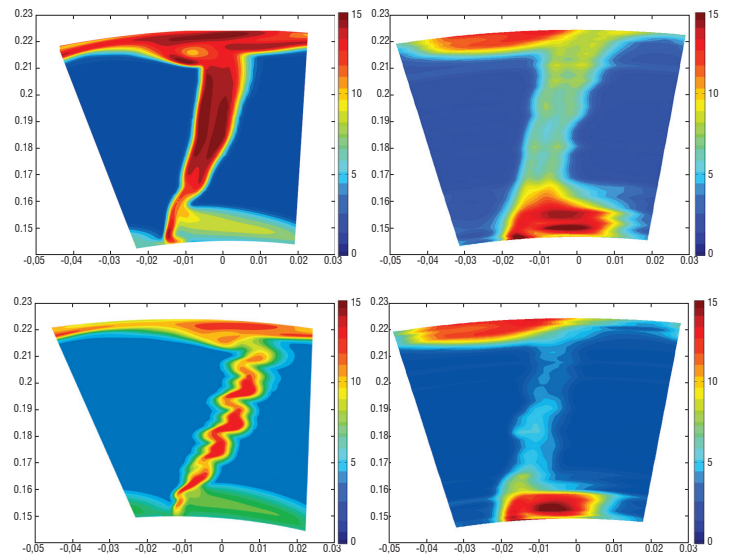


Figure 7 – Blade channel turbulent intensity plots provided by RANS-SST (left) and experiment (right): baseline (top) and blowing (bottom) cases

The LES simulation is useful to capture unsteady phenomena, as can be seen in figure 8, showing a snapshot of Mach number and Q-criterion isosurface (with/without blowing). While both computations show a separation with production of turbulent structures occurring on the suction side of the blade, separation seems to be much less massive in the blowing case. Downstream from the rotor, the turbulent structures are also smaller and restricted to a thinner wake when blowing is active. This phenomenon is highlighted in figure 9, related to the flow near the blowing slit, obtained by an average of the LES solution during a five rotor blade passage, which reveals a strong blowing effect that tends to delay the separation and reattachment points of the boundary layer almost up to the blowing slit. The turbulence kinetic energy in the blade wake region computed from velocity fluctuations during the five rotor blade passage is plotted in figure 10, for the baseline and blowing cases. A strong reduction in the turbulence kinetic energy can be clearly seen when the blowing is active.

These LES predictions were carefully checked by comparing the relevant averaged fields to those provided by RANS at the same spanwise position. Angular profiles of turbulence intensity deduced from LES (with/without blowing) at inter-stage position are plotted in figure 11 and compared to the RANS $k-\ell$ baseline solution. T_u is strongly reduced by the blowing and baseline solutions are found to be rather close to experiment, with an LES amplification that could be attributed to confined grid (quasi-2D) effects. It should be noted that the background turbulence level (about 2%) visible in figure 11 is contributing to the theta-averaged levels of T_u profiles discussed below. For reliability, we tried to obtain a similar value of this background turbulence level between RANS and measurements at the inlet boundary condition, as shown by the comparison addressed in figure 12.

Finally, the radial profiles of T_u obtained from a circumferential averaging of CFD solutions at the hot-wire plane are compared to the experimental values (blade passage trigger average) in the baseline case in figure 13, showing the best agreement for the RANS-SST model. Blowing efficiency provided by the USI RANS is found to be comparable to the measurements in terms of T_u reduction (figure 13, bottom). As already observed in figures 6 and 7, a strong turbulence activity is measured in the vicinity of the hub, attributed to a flow separation near the blade foot (laboratory test rig imperfections) and giving rise to vortex shedding not captured by RANS and not reduced by the blowing.

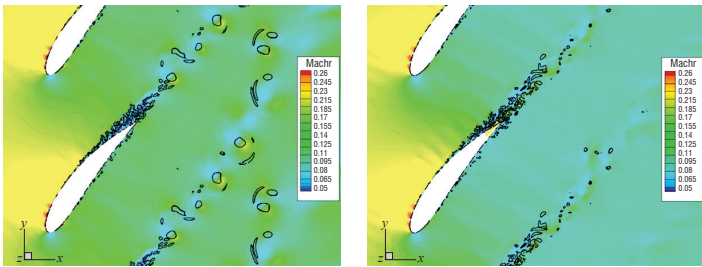


Figure 8 – Relative Mach number and iso-surface of the Q-criterion (LES snapshot): Baseline case, left, and blowing case, right

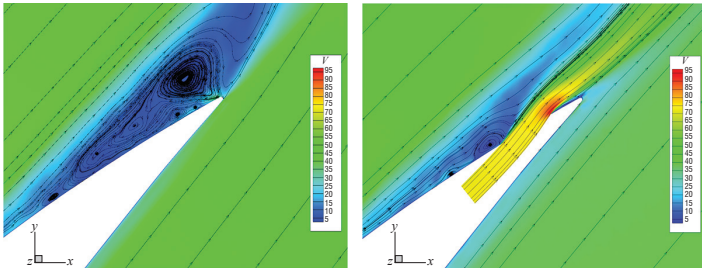


Figure 9 – LES-averaged relative velocity amplitude and streamlines near the blowing slit, without (left) and with (right) blowing

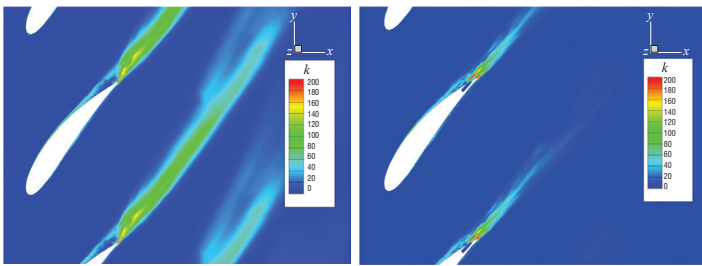


Figure 10 – Turbulence kinetic energy (m^2/s^2) from LES velocity fluctuation averaging: Baseline case, left, and blowing case, right

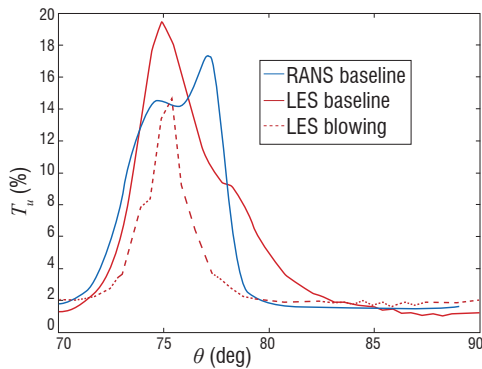


Figure 11 – LES T_u profiles compared to RANS $k-l$ at mid-span and hot-wire axial position

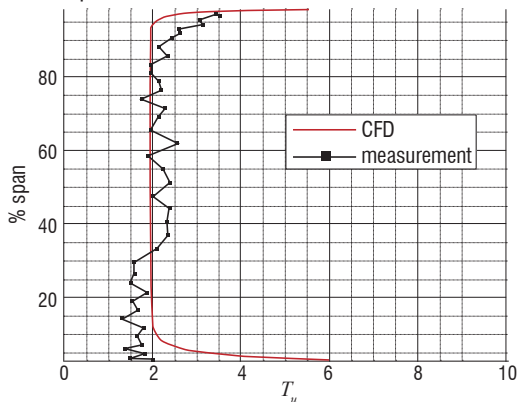


Figure 12 – T_u intensity (%) provided by RANS $k-l$ compared to measurement at the inlet

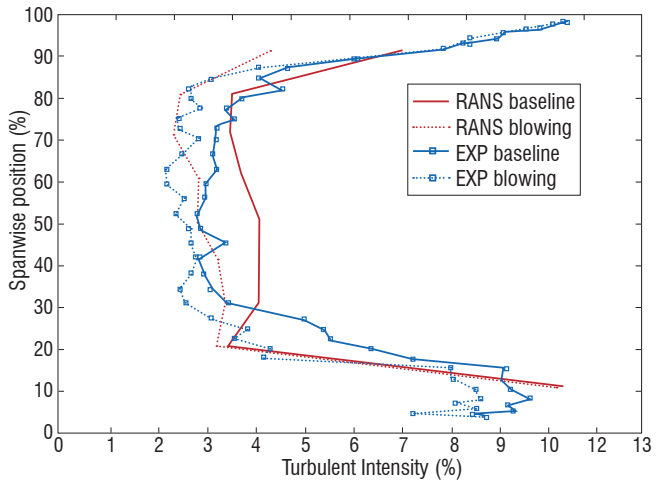
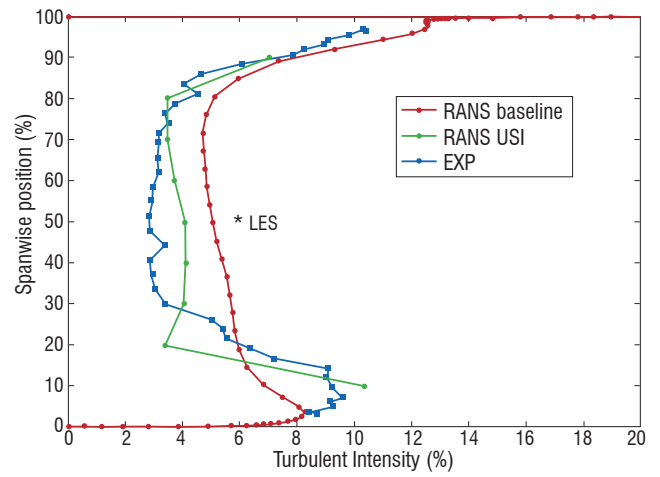


Figure 13 – T_u radial profiles: CFD vs. experiment in the baseline case (top), and blowing vs. baseline (bottom)

Turbulent velocity spectra and correlation scales

LES simulations data is post-processed, in order to assess the turbulent velocity spectra and correlation scales. PSD of the upwash velocity component ($S_{u_n u_n}$ in (4)) calculated at the inter-stage for the baseline and blowing cases are compared in figure 14 to the Von-Karman spectra (used in (3)). Slopes are similar, but a hump over a wide frequency range can be observed in the LES solutions. The streamwise 0-time shift cross-correlation function (applied to the streamwise velocity component) is compared for baseline case to the theoretical Gaussian solution [11] in figure 15 top, showing a very good agreement. The integral scale λ (deduced by integration over x) is found to be close (at mid-span) to the RANS-based solutions plotted in figure 15 bottom. RANS-based solutions are obtained from a circumferential average of the integral length scale, directly extracted from the CFD for the Onera result, because this length is a transported quantity of the $k-l$ turbulence model. Turbulent (streamwise) velocity spectra measured by hot-wire probes at 74% and 44% span are plotted in figure 16 top and bottom, respectively. These are compared to the LES solution scaled in level (-10 dB) and overplotted in figure 16 top, showing very close attenuation slopes and similar trends of blowing effects at 74%. However, blowing at 44% is much less efficient, with a level increase for frequencies beyond 4 kHz. Thus the OASPL obtained with blowing for this radial station would be just slightly lower than for the baseline case. A similar tendency for measured turbulence intensity profiles can be observed in figure 13, showing a lower level reduction around 45% span (discarding the spurious baseline oscillating point), compared to 75% span. The rise of turbulent velocity levels beyond 4 kHz (figure 16 bottom) should have a hard impact

on the noise level in this frequency range, as will be discussed in following section. The numerous peaks visible in the red spectra when the blowing is active (whereas only expected BPF tones are present without blowing) should also be noted. These might be attributed to small blowing jet variations from blade-to-blade (non-homogeneous wake filling), giving rise to multiple pure tones (rotor rotation harmonics). Such extra tones were pointed out in reference [4], when investigating alternate blade blowing.

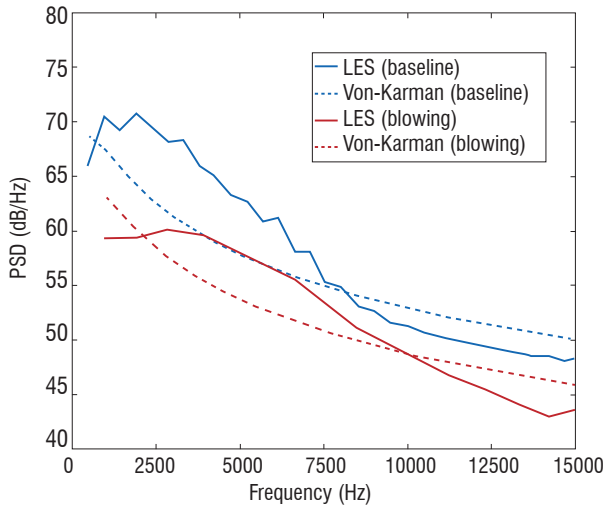


Figure 14 – PSD of upwash turbulent velocity resulting from LES and Von-Karman model

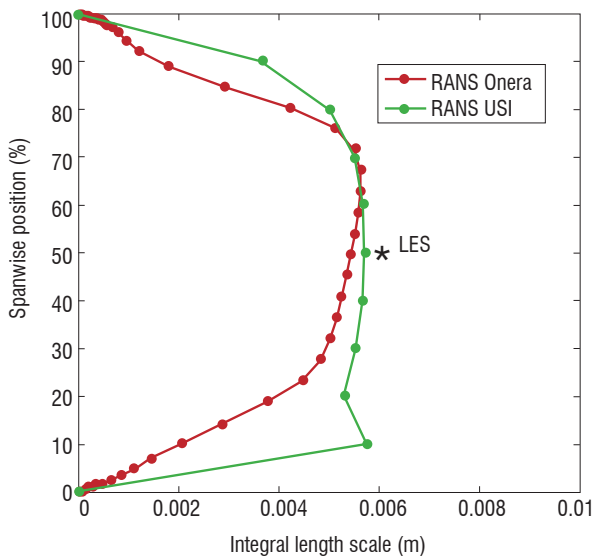
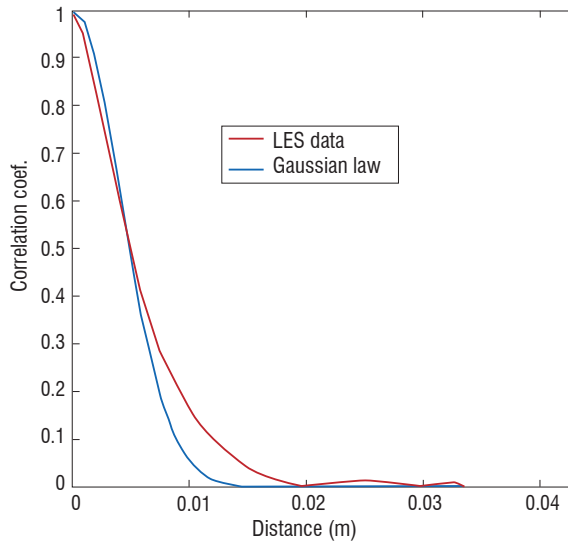


Figure 15 – LES-based streamwise correlation function (top) and integral length scale issued from RANS and LES (bottom)

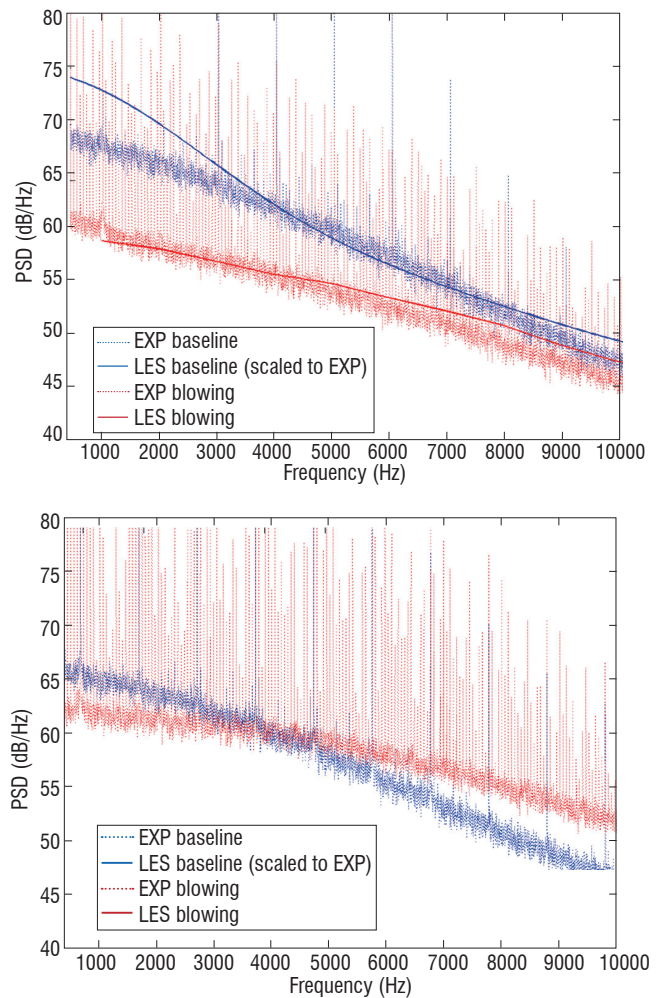


Figure 16 – PSD of streamwise turbulent velocity at 74% span (top) and at 44% span (bottom)

Assessment of sound power level broadband noise reduction

Previous RANS and LES analyses are used to estimate the PSD of acoustic pressure in the outlet duct (observer at outer wall), as shown in figure 17 for the baseline case. The LES-based prediction is achieved by applying a basic scaling correction $10 \log(L_{span} / L_{strip})$ on the sound pressure level (SPL). A satisfactory agreement is obtained for the RANS-based solutions, whereas the LES-based spectrum is over-predicted (certainly due to the quasi-2D approach restrictions). However, the frequency slope using LES seems better appraised. Finally, PSD of acoustic power (PWL spectra) using RANS-SST and LES input data are presented and compared in figure 18 top. Sound power (obtained by integrating acoustic intensity along the duct section) is more suited than sound pressure to estimate the acoustic performance of the TEB, and calculated PWL spectra have been smoothed for clarity. As expected from turbulent wake analyses, significant reductions are observed in the computation results, with relative level attenuations that are twice as large for LES compared to RANS (about 7 dB vs. 3.5 dB max), but with quite similar behavior with respect to frequency. This must be related to the experimental SPL spectra, measured by a microphone at the casing wall, in figure 18 bottom. Unfortunately, experimental results do not show any noise reduction, nor for the tones (see the non-filtered spectra), and moreover highlight a broadband level increase for frequencies beyond 4 kHz. This sound increase at high frequencies is certainly related to the rise of turbulent velocity spectra already observed from the hot-wire probe results at 44% span (figure 16 bottom). This is quite disappointing, since numerical simulations suggested significant acoustic performances of this TE blowing device, confirming the previous published results from NASA Glenn tests [3,4]. A few possible explanations of this test failure are addressed in the last section.

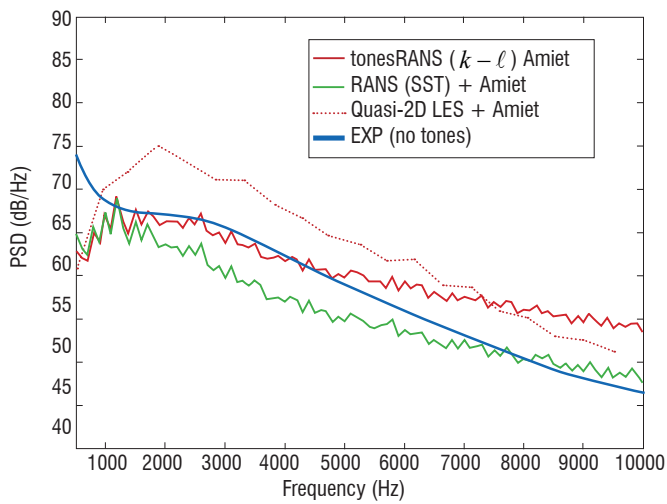


Figure 17 – SPL spectra (baseline) resulting from calculations and experiment

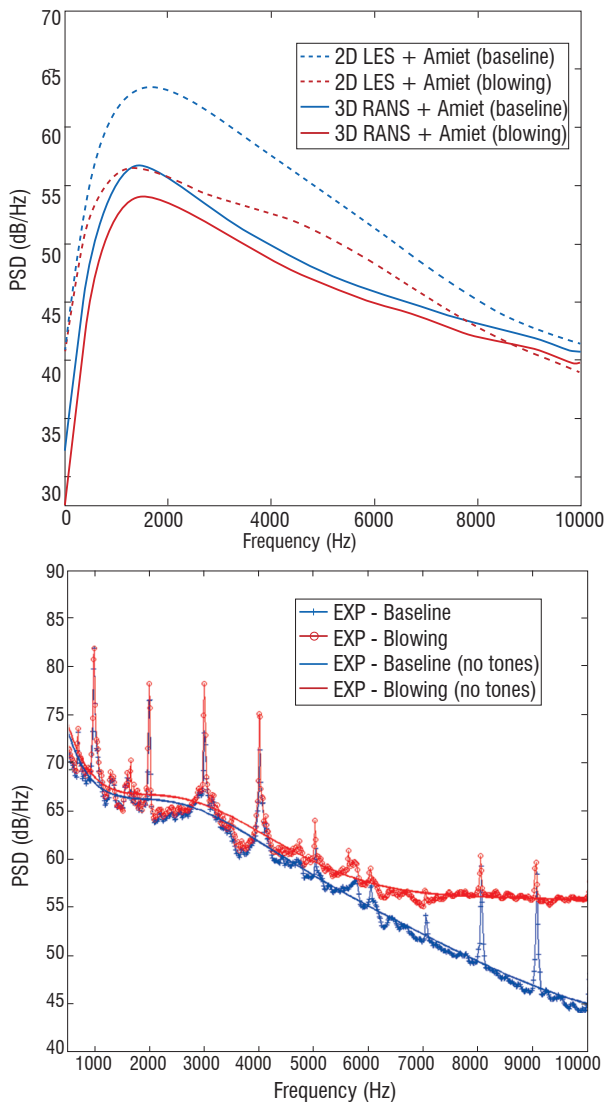


Figure 18 – Blowing effect on broadband noise spectra PWL predictions (smoothed, top) and SPL measurements (bottom)

Possible explanations of noise reduction failure in the experiments

Regarding CFD data and hot-wire probe analyzes, three main reasons can be argued for observing no noise reduction in the experiments:

- This laboratory axial compressor rig is characterized by intense turbulence structures in the vicinity of the hub and the casing, which largely contribute to the RSI broadband noise and are poorly affected by the blowing. The blowing mass flow rate was optimized assuming no separated flows at the blade foot and thus under-predicting these 3D effects in the spanwise direction. TE blowing in this test rig is certainly efficient with respect to turbulent wake reduction away from these regions. This decrease in the turbulent wake intensity is balanced by the interaction sources near the hub and casing. Similar spanwise dependency has been noticed for the velocity defects (reduction at 75% and overshoot at 45% span), limiting the tone noise reduction also;
- A non-homogeneous wake filling from blade-to-blade is suspected from rotor-clock average analyzes, revealing non fully periodic wakes in the $(r-\theta)$ planes and the presence of numerous tones in the hot-wire spectra when the blowing is active. This may also be responsible for minimizing the efficiency of the blowing, assumed to be fully homogeneous in the simulations;
- Due to the small size of the slits, the blowing jet speed is very high and jet mixing velocity fluctuations captured by hot-wire measurements at some radial positions may contribute to self jet noise, particularly at medium and high frequencies, as shown by the sound spectra.

Conclusions

A comprehensive study of turbofan broadband noise reduction using a trailing edge blowing device has been carried out numerically and experimentally in a laboratory axial compressor stage rig. The blowing design and optimal settings were obtained through extensive RANS computational studies. 3D RANS simulations have been supplemented by quasi-2D LES, in order to better assess the turbulent characteristics of the flow, and CFD post-processed data has been used as input to an Amiet-based acoustic calculation. Wake analyses have shown relevant reductions in the velocity defect and turbulent intensity, in good agreement with the hot-wire measurements performed in the inter-stage plane. These are responsible for significant SPL attenuations in the outlet duct spectra (up to 3.5 dB for RANS-based and up to 7 dB for LES-based solutions) with a similar response to frequency, which lets this methodology appear reliable. However, the acoustic measurements have not revealed any acoustic performance of the blowing (moreover, some noise increase was detected at high frequencies). This mismatch has been discussed at the end of the paper and can be attributed to a strong turbulence activity in the test rig duct wall hub and to a non-homogeneous wake filling from blade-to-blade. The contribution of mixing jet sources not considered in these simulations is also suspected ■

Acknowledgements

This work was supported by the European Commission (FLOCON).

References

- [1] J.M. BROOKFIELD and I.A. WAITZ – *Trailing-Edge Blowing for Reduction of Turbomachinery Fan Noise*. Journal of Propulsion and Power, vol. 16, n°. 1, pp. 57-64, 2000.
- [2] D.L. SUTLIFF, D.L. TWEEDT, E.B. FITE and E. Envia – *Low Speed Fan Noise Reduction with Trailing Edge Blowing*. NASA/TM-2002-211559, 2002.
- [3] D.L. SUTLIFF – *Broadband Noise Reduction of a Low-Speed Fan Noise Using Trailing Edge Blowing*. NASA/TM-2005-213814 and AIAA-2005-3028, 2005.
- [4] R.P. WOODMARK, E.B. FITE and G.G. PODBOY – *Noise Benefits of Rotor Trailing Edge Blowing for a Model Turbofan*. AIAA-2007-1241, 2007.
- [5] V. JURDIC, A. MOREAU, P. JOSEPH, L. ENGARDT and J. COUPLAND – *A Comparison between Measured and Predicted Fan Broadband Noise Due to Rotor-Stator Interaction*. AIAA-2007-3692, 2007.
- [6] M.L. LANGFORD, C. MINTON, W.F. NG, R.A. BURDISSO and C. HALASZ – *Fan Flow Control for Noise Reduction Part 3: Rig Testing of Optimal Design*. AIAA-2005-3027, 2005.
- [7] M. KOHLHAAS and T. CAROLUS – *Trailing Edge Blowing for Reduction of Rotor-Stator Interaction Noise: Criteria, Design and Measurements*. ISROMAC-14, Honolulu (USA), 2012.
- [8] ANSYS – *Ansys CFX-Solver, Release 10.0: Modelling*. Canonsburg, Pennsylvania, 2005.
- [9] B.R. SMITH – *The Near-Wall Model for the $k - \ell$ Two Equation Turbulence Model*. AIAA-94-2386, 25th Fluid Dynamics Conference, Colorado Springs (Colorado), 1994.
- [10] J. RIOU, S. LÉWY and S. HEIB – *Large Eddy Simulation for Predicting Rotor-Stator Broadband Interaction Fan Noise*. Inter-noise 2007, Istanbul, August 2007.
- [11] G. ASHCROFT and D. NURNBERGER – *A Computational Investigation of Broadband Noise Generation in a Low-Speed Axial Fan*. AIAA-2009-3219, Miami, Florida, 2009.
- [12] F. NICOU and F. DUCORS – *Subgrid-Scale Stress Modelling Based on the Square of the Velocity Gradient*. Flow Turbulence and Combustion, vol. 62(3), pp. 183-200, 1999.
- [13] R. K. AMIET – *High-Frequency Thin Airfoil Theory for Subsonic Flow*. AIAA Journal, 14(8), 1976.
- [14] G. REBOUL, C. POLACSEK, S. LÉWY and S. HEIB – *Ducted-fan Broadband Noise Simulations Using Unsteady or Averaged Data*. Inter-noise2008, Shanghai, China, 2008.
- [15] D.A. LYNCH, T.J. MUELLER and W.K. BLAKE – *A Correlation Length Scale for the Prediction of Aeroacoustic Response*. AIAA-2002-2569, 2002

Acronyms

AAPL	(Aero-Acoustic Propulsion Laboratory)
ANCF	(Advanced Noise Control Fan)
CFD	(Computational Fluid Dynamics)
GGI	(General Grid Interface)
LE	(Leading Edge)
LES	(Large Eddy Simulation)
LSWT	(Low Speed Wind Tunnel)
OASPL	(Over All Sound Pressure Level)
OGV	(Outlet Guide Vanes)
PSD	(Power Density Spectrum)
PWL	(sound PoWer Level)
RANS	(Reynolds-Average Navier-Stokes)
RSI	(Rotor Stator Interaction)
SPL	(Sound Pressure Level)
SST	(Steady State Turbulence)
TEB	(Trailing Edge Blowing)
USI	(University of Siegen)
WALE	(Wall Adapting Local Eddy-viscosity)



Cyril Polacsek graduated from the Ecole Nationale Supérieure d'Ingénieurs de Poitiers (ENSIP) in 1989, with a Masters Degree in aeroacoustics and signal processing. He started his career at Onera as a test engineer (rotorcraft test campaigns in S1-Modane wind tunnel facilities) and became a specialist in source modeling and numerical simulations related to turbomachinery noise. He is now in charge of turbofan noise activities in the "CFD and Aeroacoustics" Department.



Raphaël Barrier graduated from the École Centrale de Marseille and received a Masters Degree in mechanical and aerospace engineering at the Ecole Centrale Paris in 2005. An engineer at Onera since 2006, he is in charge of CFD studies and software development concerning analysis and design for turbomachinery components. He is also in charge of the technical and scientific aspects of the turbomachinery related studies in the Applied Aerodynamics Department.



Michael Kohlhaas graduated in 2009 from the University of Siegen, where he obtained his Diploma degree in Mechanical Engineering. Since 2009, he has been working as a doctoral student in the Turbomachinery Group of the Fluid und Thermodynamics Institute (Institut für Fluid und Thermodynamik, IFT) in Siegen. His current activities involve the reduction of rotor-stator interaction noise by trailing edge blowing.



Prof. Thomas Carolus is head of the Turbomachinery Group at the Fluid and Thermodynamics Institute (Institut für Fluid und Thermodynamik, IFT) of the University of Siegen, Germany. He received his Diploma, Master and Ph.D. degrees from the Universität (Technische Hochschule) Karlsruhe and the Georgia Institute of Technology in Atlanta, USA. Before joining the University of Siegen, he was senior research engineer for the German automotive supplier Bosch.



Philip Kausche studied Aeronautics and Astronautics at the Technical University of Berlin and graduated in 2008. He wrote his diploma thesis in the Engine Acoustics department at the German Aerospace Center (DLR) in Berlin. Since then, he has worked there as a research scientist on several European projects. Currently, he is working on the completion of his dissertation, which is about noise control in a turbomachine.



Antoine Moreau studied in Toulouse at the Ecole Nationale Supérieure d'Ingénieurs en Construction Aéronautique (ENSICA) and obtained his degree in Aerospace Engineering in 2005. Since then, he has been working at the Engine Acoustics Department of the German Aerospace Center (DLR) located in Berlin. His research is focused on fan and compressor acoustics and the development of low-noise aerodynamically efficient designs, based on experiments and theoretical prediction methods.



Fritz Kennepohl received his mechanical engineering diploma at the Technical University of Braunschweig in 1978. Since then he has been working for MTU Aero Engines in various positions, on acoustic design of aeroengine components, development of noise prediction methods, analysis of measurements, etc. His scientific focus has been on the generation and reduction of turbomachinery noise and particularly turbine noise. He retired in 2013, after the end of the European Research project FLOCON.